U.S. Department of Transportation

OST-R CRS&SI Technologies Program – Phase III –

Research Title: Multi-modal Remote Sensing System (MRSS) for Transportation Infrastructure Inspection and Monitoring

Contract Number: OST-RS-11-H-UML

Final Report *(Draft)*

Reporting Period: 07/15/2011 ~ 12/14/2013

PI Name: Tzuyang Yu

Program Manager Name: Caesar Singh

TABLE OF CONTENTS

GLOSSARY

MRSS: Multi-modal Remote Sensing System / CWIR: Continuous Wace Imaging Radar / DIC: Digital Image Correlation / FOS: Fiber Optic Sensors / BOTDR: Brillouin Optical Time Domain Reflectometry / BOTDA: BrillouinOptical Time Domain Analysis / FBG: Fiber optic Bragg Grating

EXECUTIVE SUMMARY

In this final report draft, our research results during the project period are highlighted and summarized. Detailed description of our research activities is documented in our submitted quarterly reports. The results reported in this Final Report draft are categorized by Project Deliverables, as organized in our proposal. Although the project has officially ended on December 14, 2013, the research team still continued collecting field data from the bridges in Lowell (MA) and Chicago (IL) and modifying the proposed MRSS technology. We are also in the process of applying two patents, with the help of the Office of Commercial Ventures and Intellectual Property (CVIP). Our industry partner (Trilion Quality Systems) has created a new product line for the prototype MRSS technology and is working with few state DOTs to promote the use of the MRSS technology.

I — TECHNICAL STATUS

1. **Project kick-off meeting** – Held on 08/26/2011 at UML (Trustees Room, North Campus), with all PIs from UML (Yu, Niezrecki, Avitabile, Faraji, Kachen), Trilion Quality Systems (Tyson, Schmidt), LR Tech (Lai, Ren), HNTB (Carney, call-in) and the Dean of Engineering Dr. John Ting.

Fig. 1. Project kick-off meeting on 08/26/2011 at UML

2. **Project website** – Launched on 09/18/2011 at http://tyu.eng.uml.edu/usdot%5Fmrss/.

   A project logo is also created for future use in commercialization, as shown in Fig. 2.

Fig. 2 MRSS project logo (designed by Yu)

Screen print of the project website is shown in Fig. 3.

Fig. 3. Project website (first page)

3. **Project Advisory Board (Technical Advisory Council) meetings** – Held on 09/27/2011, 06/17/2012, 02/26/2013, with MassDOT (Alex Bardow) and PennDOT (Tom Macioce), ConnDOT (Scott Hill). Other TAC members were briefed via electronic reports.

4. **Hardware design of CWIR using array beamforming techniques** – Reported in Y1Q1 Quarterly Report. Array beamforming results were simulated to identify the design specs for optimal performance. Fig. 4 shows the predicted radiation pattern using beamforming techniques. Fig. 5 shows the first generation of CWIR prototype.

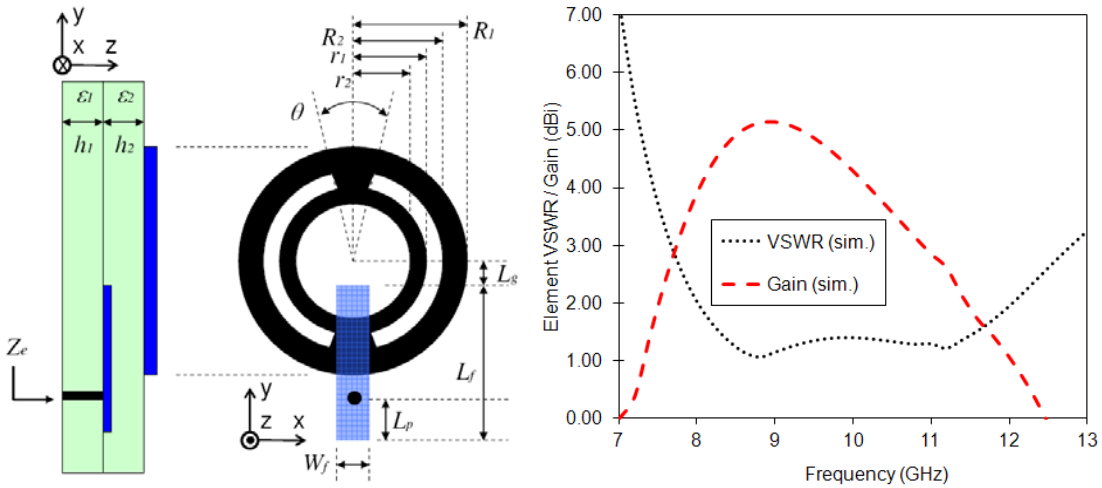

Fig. 4 (a) Geometry of the antenna element; (b) the VSWR and radiation gain of the X-band antenna element.

(a) Radar with Laptop (b) Close look of radar system

Fig. 5 CWIR prototype – First generation

5. **Numerical simulations (e.g., Method of Moments, Finite Difference Time Domain) to estimate radar radiation patterns** – Method of Moments (MoM) and Finite Difference Time Domain (FDTD) were used to simulate the radar response (radiation pattern) of the proposed antenna and construction material targets. Fig. 6 shows the simulated radiation patterns of the CWIR antenna at 8, 10, and 12 GHz.

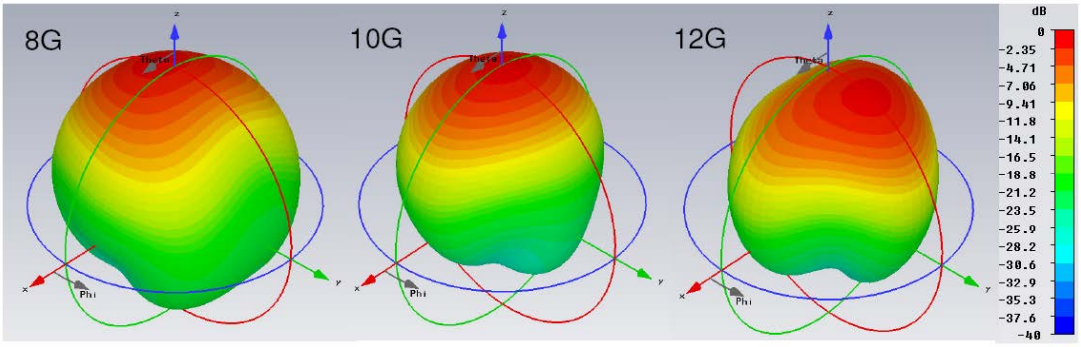

Fig. 6 Simulated radiation patterns of the X-band antenna element at 8 GHz, 10 GHz, and 12 GHz.

Fig. 7 shows the simulated radiation pattern of a metal plate at 1 and 10 GHz. The same metal plate is also physically manufactured.

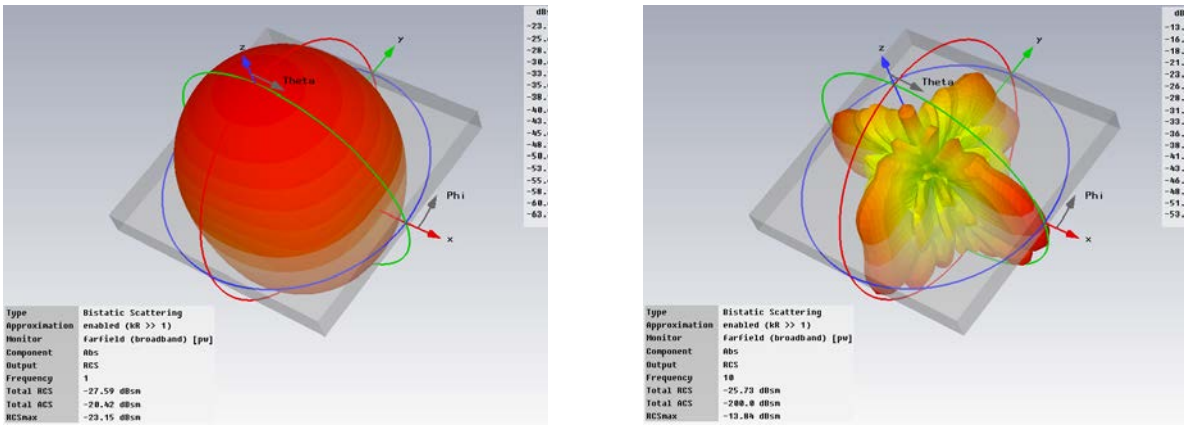

(a) (b)

Fig. 7 Radiation patterns of a metal plate at (a) 1 GHz and (b) 10 GHz.

6. **Design and manufacturing of a steel beam and a reinforced concrete beam** – Schematics and a photo of the steel beam specimen are shown in Figs. 8 and . Schematics and a photo of the reinforced concrete beam specimen are shown in Figs. 10 and 11.

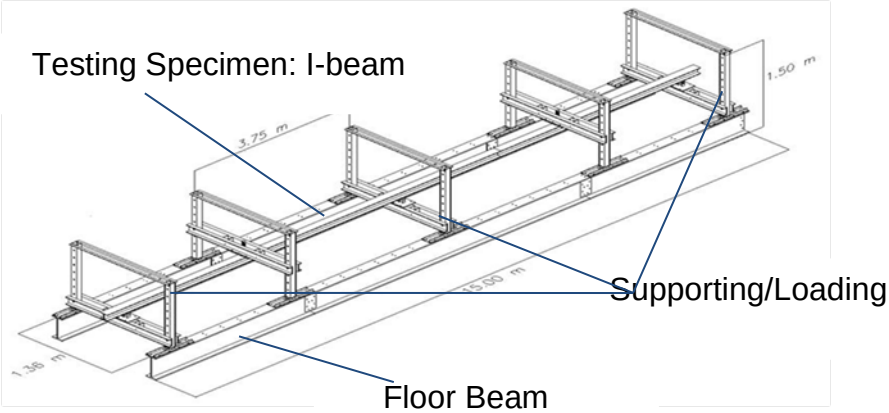

Fig. 8 Schematics of the steel beam specimen

Fig. 9 Fabricated steel beam specimen

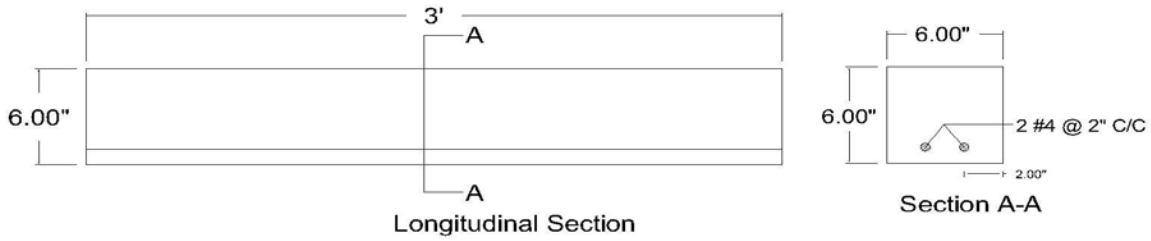

Fig. 10 Schematics of the reinforced concrete beam specimen

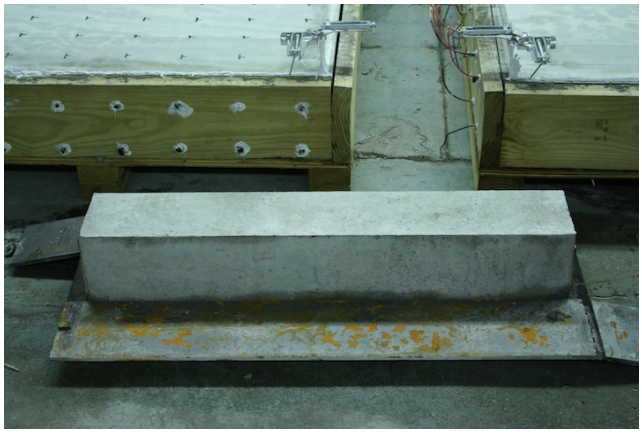

Fig. 11 Manufactured reinforced concrete beam specimen

7. **Numerical simulation of returned radar signals to identify damage types, location and damage levels by numerical simulation, using designed radar**

system – Six concrete specimens with different damage types were considered in the numerical simulation. Fig. 12 shows the design of these six specimens and Figs. 13 and 14 provide the numerically simulated return radar signals using 10 GHz and 12 GHz radar signals.

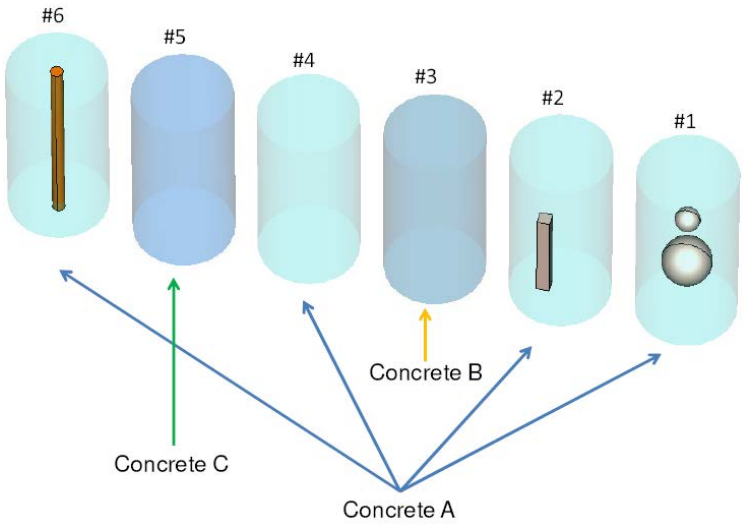

Fig. 12 Six concrete specimens with different damage types

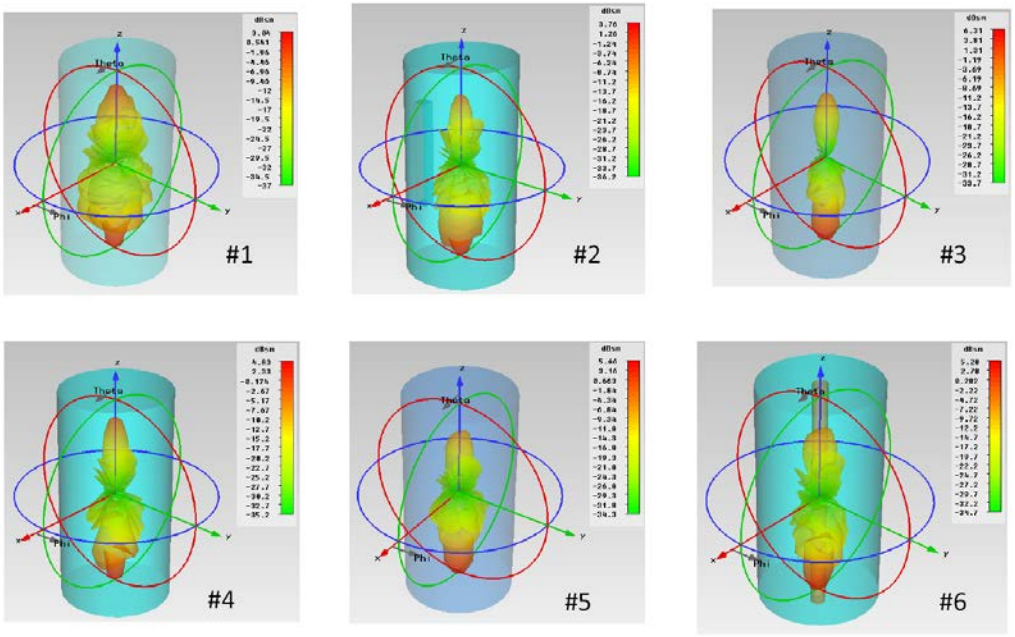

Fig. 13 RCS patterns of all specimens at 10 GHz (unit: dBsm)

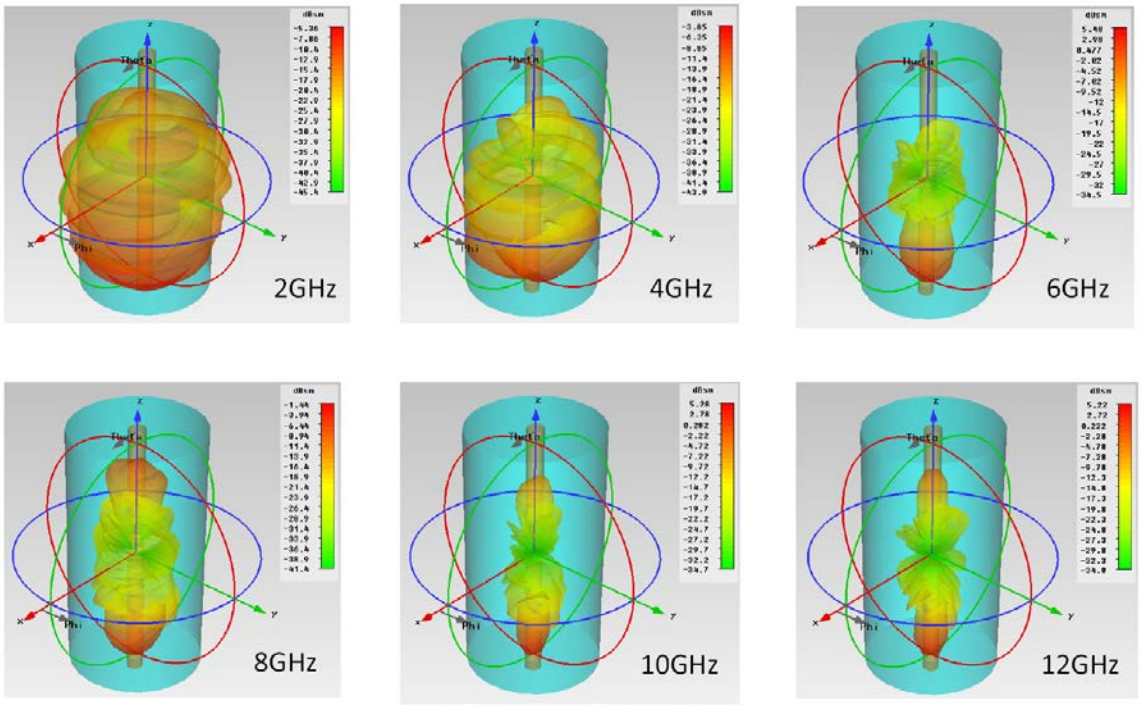

Fig. 14 RCS patterns of Specimen #6 at 2, 4, 6, 8, 10, and 12 GHz (unit: dBsm)

8. **Laboratory radar testing for calibrating radar elements** – In order to characterize the radar antenna in a noise-free environment, an electromagnetic anechoic chamber is necessary. We designed and built an anechoic chamber for the X-band (8~12 GHz) and Ku-band (12~18 GHz) radar measurements. Fig. 15 shows the constructed anechoic chamber located in the Department of Civil and Environmental Engineering at UML, in Falmouth Hall Room 104. Experimental configuration of radar tests is provided in Fig. 16. Fig. 17 shows the laboratory radar test results using a standard reflector. In Fig. 17, the x axis is measurement frequency in MHz and the y axis is the measured scattering parameter. The standard reflector test result shows that the average of the measured scattering parameters is close to zero, as expected. Fig. 18 summarizes the results in decibels.

Fig. 15 An electromagnetic anechoic chamber at UML for testing the MRSS system

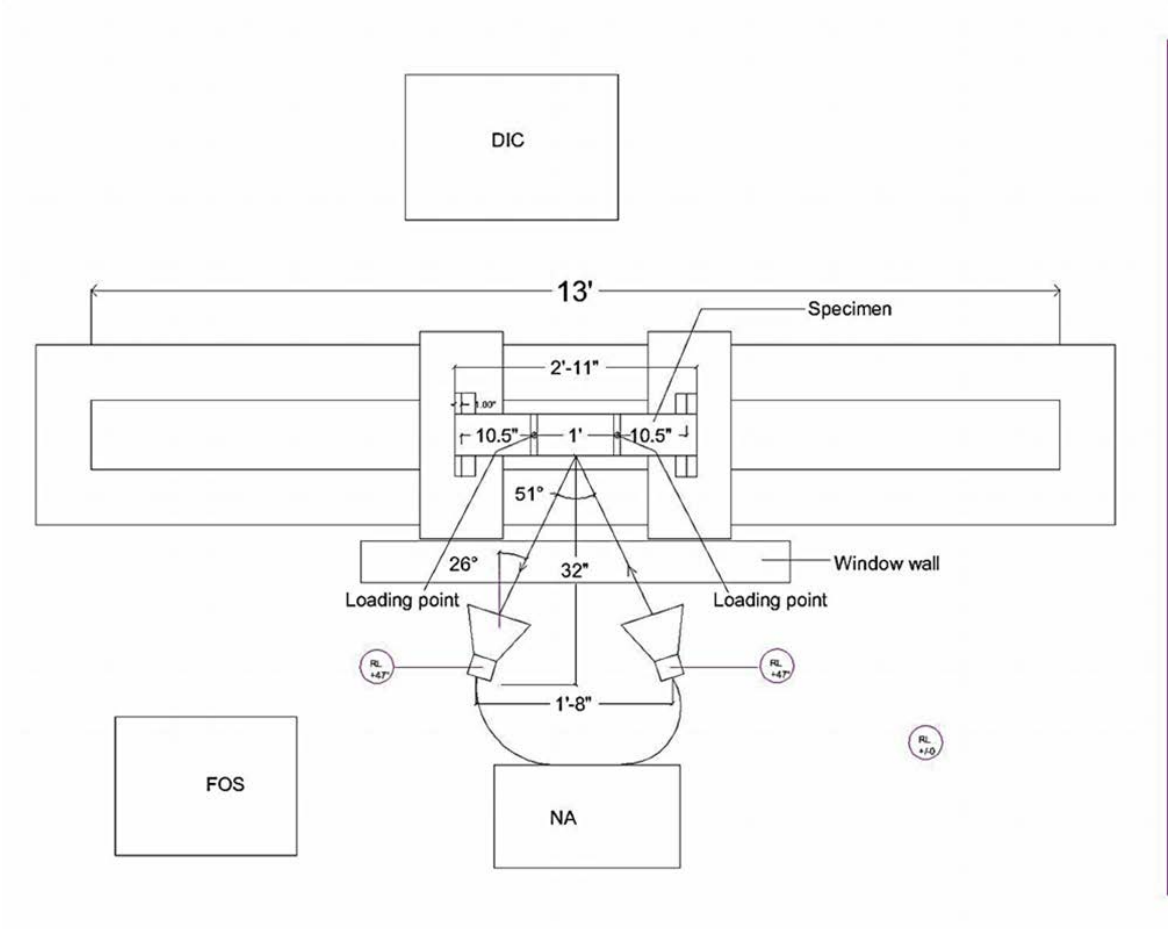

Fig.16 Laboratory radar test configuration

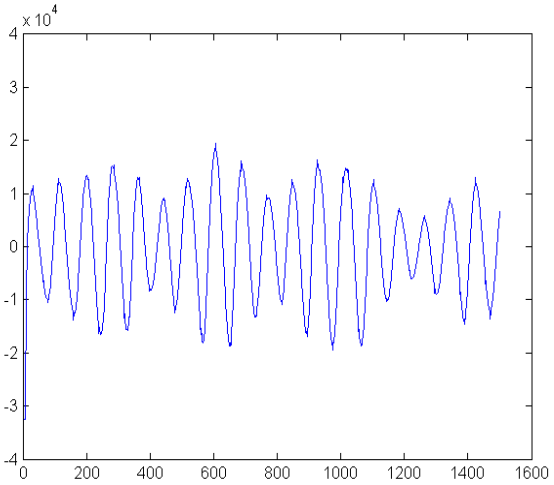

(a) Reflector at 0 meter range

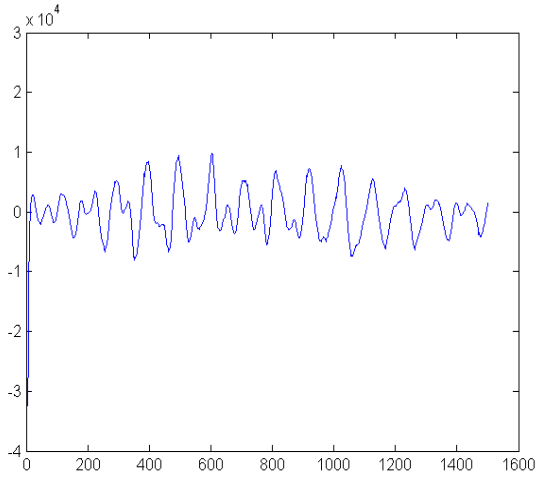

(b) Reflector at 1 meter range

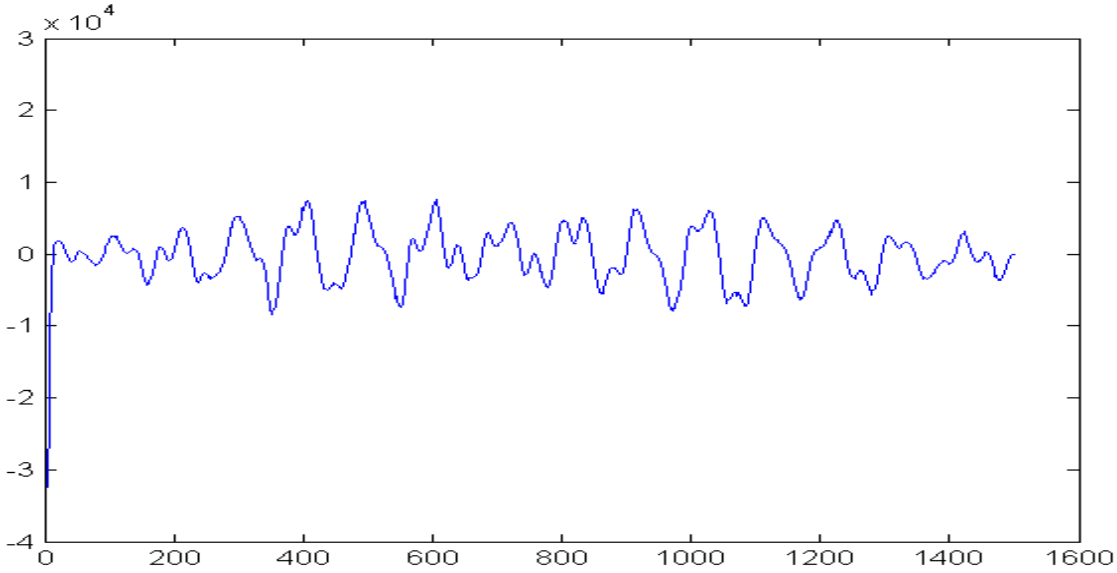

(c) Reflector at 2 meter range

Fig. 17 Laboratory radar test results using a standard reflector

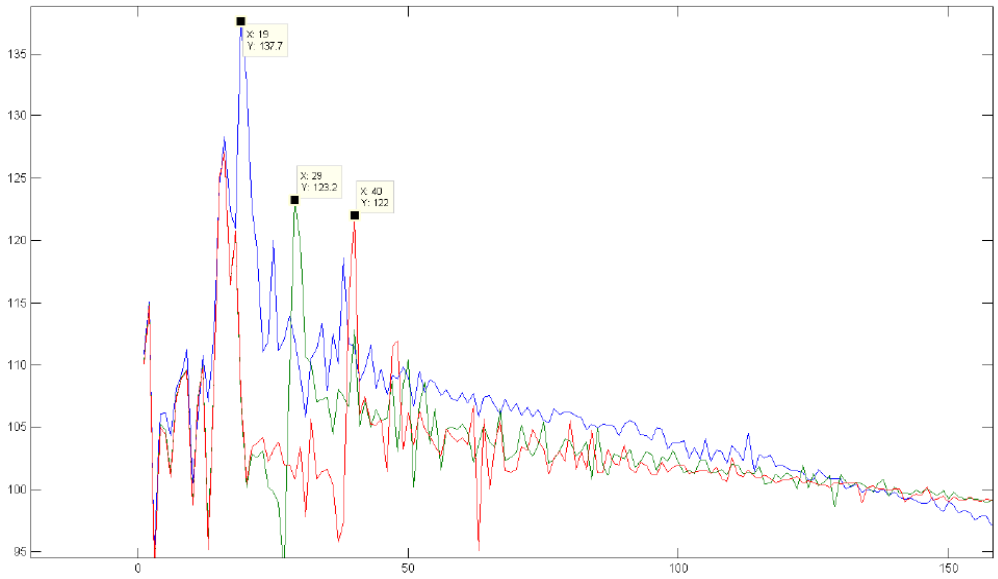

Fig. 18 Spectrum (absolute magnitude in dB) response of all the reflector test results; Mark points represent target positions at 0.1 meter, 1 meter and 2 meters

9. **Probability analysis and determination of thresholds for radar sensitivity analysis using Monte-Carlo simulation** – *(Please see a separate report on **Monte-Carlo simulation**)*

10. **Final hardware design and manufacturing of CWIR and further modifications for a portable CWIR prototype** – With the reflector test results and further simulation, the second generation (version 3) was manufactured. All versions of the CWIR are shown in Fig. 19. From version 1 (lab system) to version 2 (first generation), we eliminated one radar antenna to consider the practical constraints (coordination of two radar antennas without a fixture bar) in the field. From version 2 to version 3 (second generation) we integrated all radar components and eliminated the use of a network analyzer. ***In the field measurement using CWIR, only a***

small radar box is needed. Fig. 20 shows the final simulated radiation pattern for the CWIR prototype (version 3, second generation).

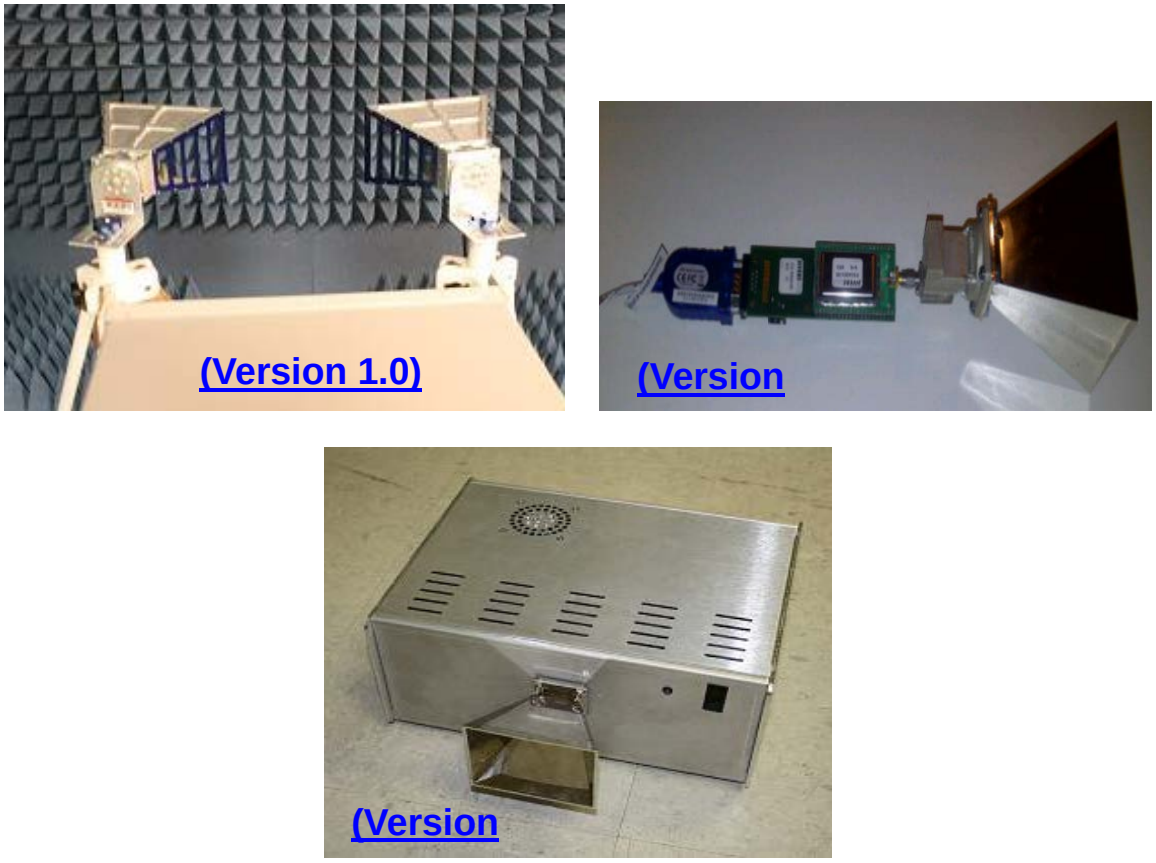

Fig. 19 Evolution of CWIR prototypes (this process shows our effort on converting a laboratory system into a commercial product)

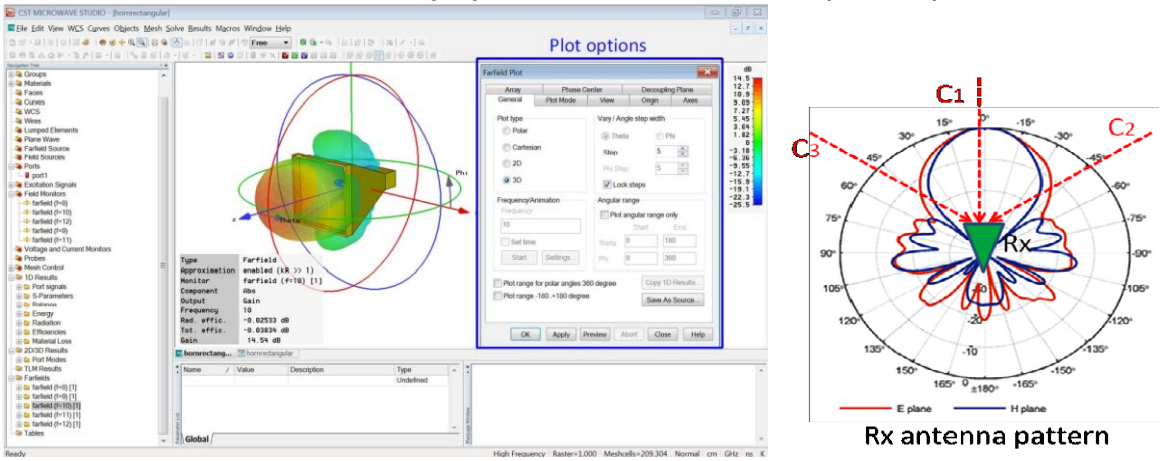

Fig. 20 Simulated radiation patterns of the CWIR antenna

11. **Laboratory experiments and modeling to establish correlation between FBG and BOTDA measurements** – *(Please see a separate report on **FOS Laboratory Tests**)*

12. **Laboratory measurements to establish correlation between CWIR and BOTDA sensors** – Fig. 21 shows two laboratory RC beam tests at UML to establish the correlation between CWIR and BOTDA. Fig. 22 shows the correlation between CWIR and BOTDA sensors. A linear relationship was found in our laboratory tests.

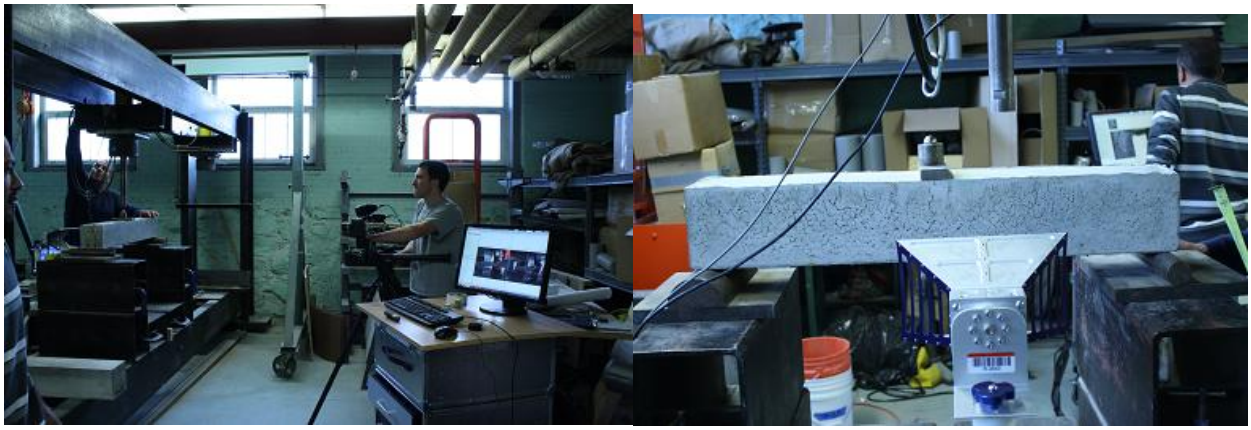

(a) First RC beam test (Three-point bending)

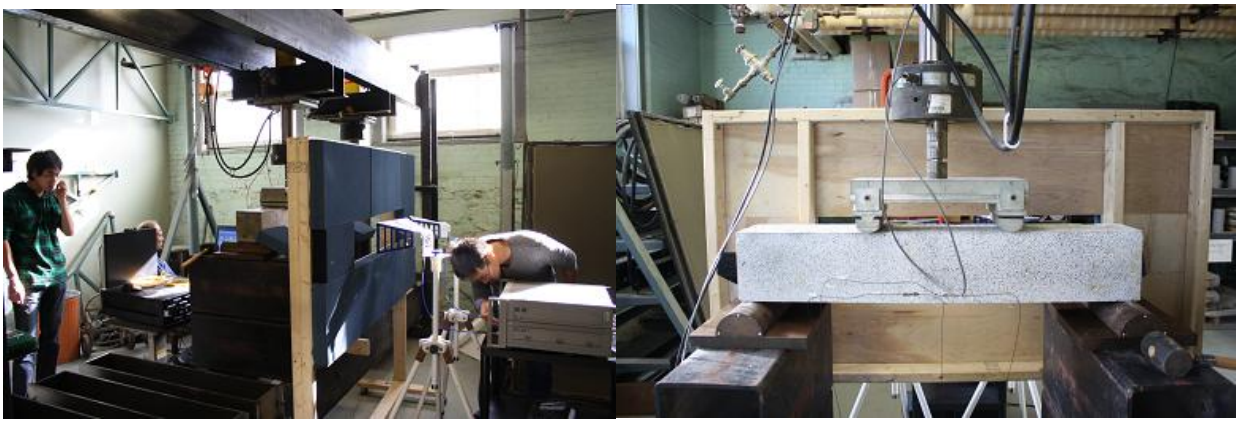

(b) Second RC beam test (Four-point bending)

Fig. 21 Laboratory measurements on a RC beam

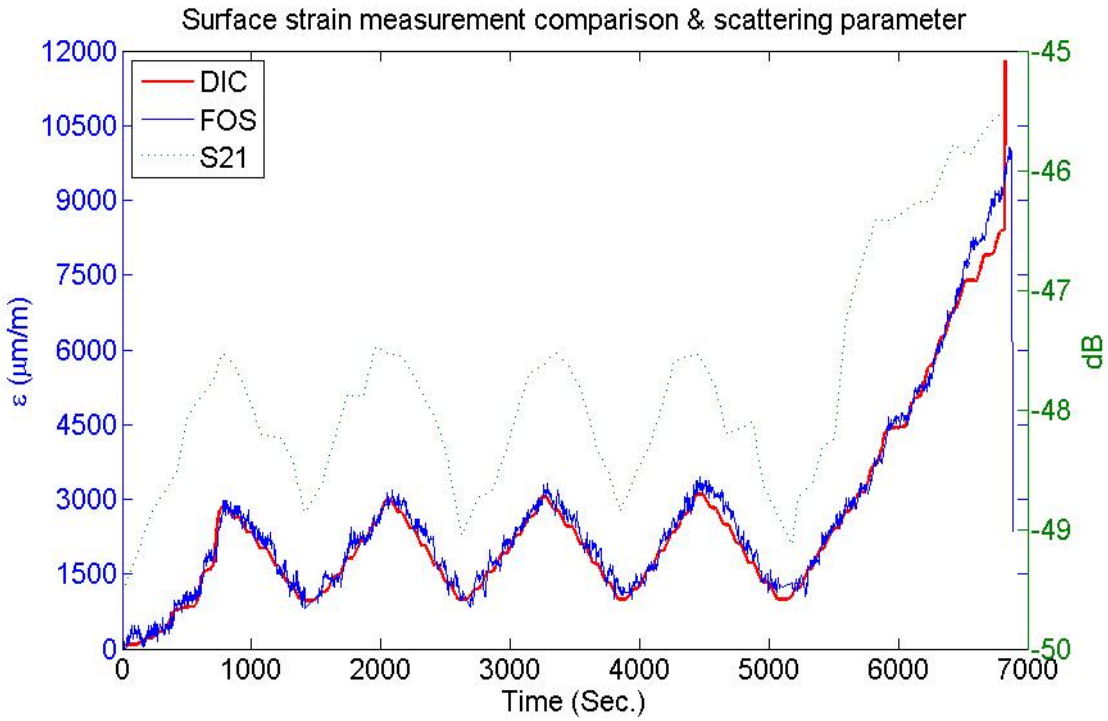

Fig. 22 Correlation between CWIR and BOTDA; the DIC measurement is also compared.

13. **Laboratory experiments relating the full field strain measurements with the distributed strain measurements by BOTDA to establish the BOTDA/FBG correlation models. Field testing for BOTDA and FBG sensors on a steel bridge and a reinforced concrete bridge** – (*Please see a separate report on **FOS Laboratory Tests**)*

14. Damage detection threshold lab tests to test the ability of CWIR and DIC to detect and quantify crack growth using accelerated aging tests and mechanical loading. – In the laboratory RC beam test, scattering parameters (S-parameters) were also measured for to correlate the concrete crack propagation with CWIR measurements. Fig. 23 shows the S-parameter curves measured by the CWIR sensor at various

concrete cracking levels. The DIC measurement of the RC beam is provided in Fig. 24, as an example to illustrate how we have successfully used DIC to predict crack propagation in concrete structures. The DIC image in Fig. 24 corresponds to one S-parameter (CWIR) curve in Fig. 23. In other words, *the CWIR measurement curve provides the radar response of the RC beam at* ***multiple frequencies****, while the DIC measurement provides the stress/strain measurements at* ***multiple locations****.*

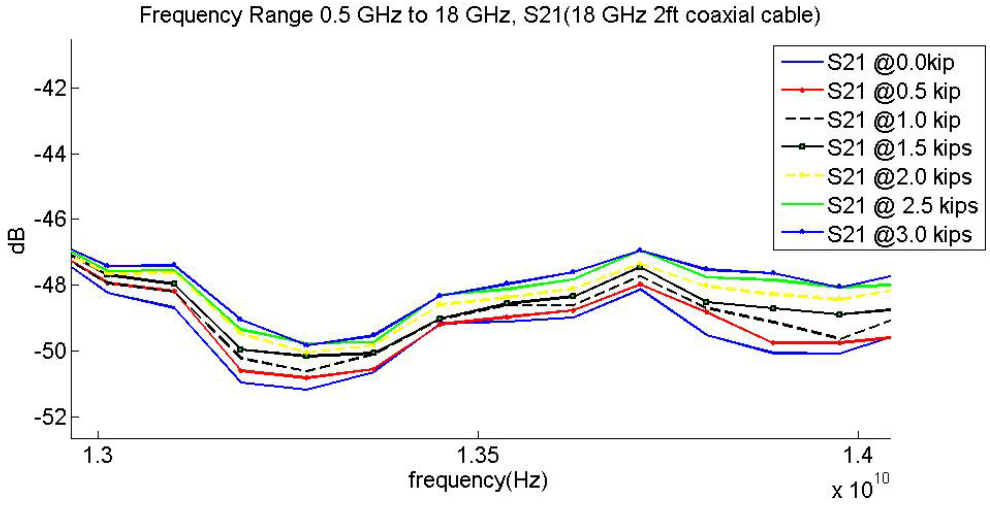

Fig. 23. CWIR measurement at various cracking levels in a RC beam

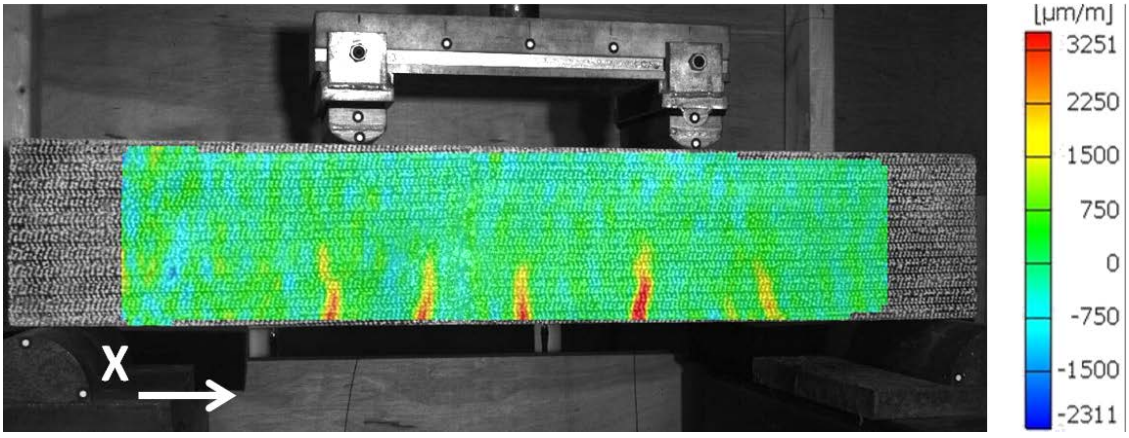

Fig. 24. DIC strain/stress measurement of the RC beam (Second RC beam test)

15. **Field tests of projected dot shape measurements in Lowell, MA, 2D image correlation testing. Core drilling for operational stress determination**. – *(Please see a separate report on **CWIR/DIC Field Tests**)*
16. **Field test and validation of MRSS at UML (Lowell, MA) and UIC (Chicago, IL). Modifications of the portable sensor of MRSS**. – *(Please see a separate report on **CWIR/DIC Field Tests**)*
17. **Present major research results the Project Advisory Board and a selected group of bridge inspectors**. – We have presented our research results to MassDOT in a visit in 2013 to Alex Bardow and his staff in the MassDOT office in downtown Boston. We also have presented our result to ConnDOT to Mr. Scott Hills in a teleconference meeting. From both meetings, we received positive feedbacks and useful suggestions.
18. **Present the results at relevant workshops or national conferences as well as to several state DOTs.** – We have presented our research work in several domestic and international conferences, including:
    - U.S. – 2012, 2013, SPIE Smart Structures/NDE, San Diego, CA (6 papers)
    - U.S. – 2013, IWSHM, Stanford, CA (1 paper)
    - Europe – 2012, Structural Faults and Repair, Edinburg, U.K. (1 paper)
19. **Project final meeting** – Project final meeting was originally scheduled on December 2013 but postponed to March 27 due to the conflicts of schedule of PIs. We will report our final meeting right after our meeting.

II — BUSINESS STATUS

We have completed all tasks and are in the process of account reconciliation. All invoices and cost shares from our Joint Venture partners (Univ. Illinois Chicago, Trilion Quality Systems, LR Technologies) have been submitted to the lead Institute (UML), and we are in the process of verifying these submissions. A less than 5% budget readjustment plan is proposed to the U.S. DOT to reflect the actual spending generated from our last phase of hardware modification and field tests of the MRSS technology.

RESEARCH FINDINGS

From our laboratory and field activities, key research findings are summarized in the following.

- **Material characterization and subsurface rebar detection using CWIR** – CWIR can identify the type of materials in both distant laboratory and distant field measurement schemes. CWIR can also identify and locate a #3 subsurface rebar inside concrete at a concrete cover of 3” from distant measurement (Fig. 25).
- **Effect of background noise on the CWIR performance** – Background noise (electromagnetic) does not affect the performance of CWIR when conducting distant measurements within 100 ft. Detectability of CWIR is not jeopardized by background noise in the field when signal-to-noise ratio (SNR) is higher than 1.5~2 in various applications. Denoising techniques are helpful in improving the detectability of CWIR in field applications.

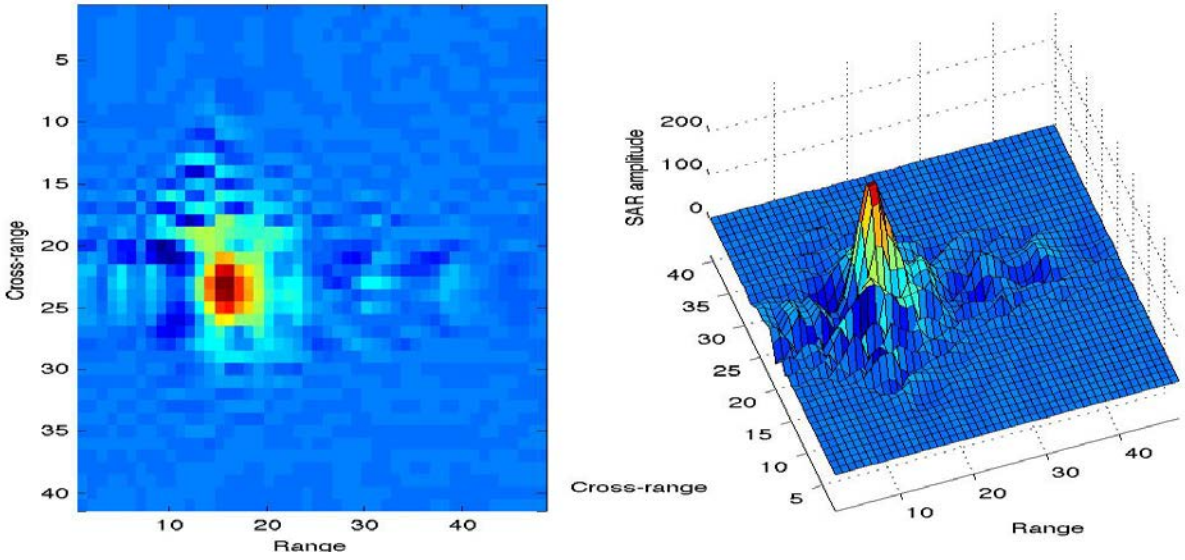

Fig. 25 Subsurface CWIR imaging of a RC cylinder

- **Long-term surface strain/displacement monitoring using DIC** – DIC is capable of monitoring the long-term displacement and reconstructing the surface stress/strain fields of reinforced concrete (RC) highway bridges, from our 9-month field measurements. Using surface stress distribution, DIC can also indicate possible cracking areas of RC bridge elements, even though there is no visible surface cracking of concrete, as shown in Fig. 26.
- **Calibration of DIC in field measurement** – Calibration and pattern deployment are important to the performance of DIC. Various pattern deployment schemes (e.g., physical painting, optical laser projecting) were investigated and tested. Optical laser projecting scheme is applicable and uses only few reference marks on the surface of structures.
- **Local and global correlation between DIC and FOS sensor** – Laboratory and field FOS strain measurements show good agreement with the DIC result,

suggesting the robustness of DIC for global strain measurement, both in the lab and in the field.

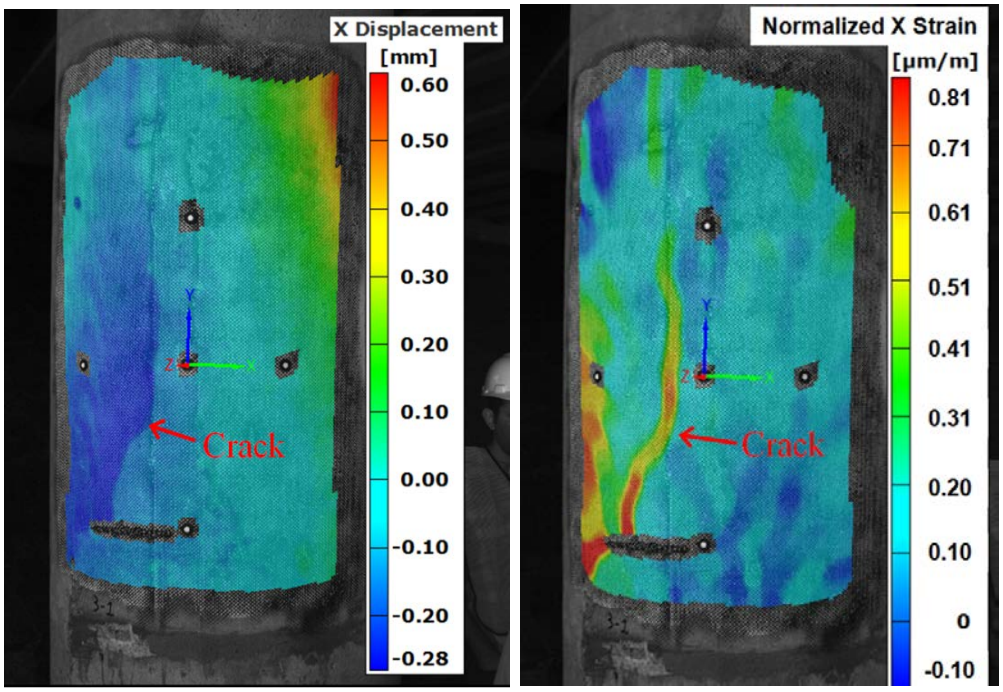

(a) X-axis displacement (b) Normalized x strain

Fig. 26 Displ. and strain of a RC highway bridge pier

- **Multi-physical coupling between CWIR, DIC, and FOS** – Multi-modal laboratory RC beam tests using CWIR, DIC, and FOS demonstrated a consistent, repeatable coupling pattern between the electromagnetic (CWIR) and mechanical responses of a RC beam. It is found that, under a given/known load, the local mechanical response (stress/strain) of a RC beam can be related to the global behavior of the beam via a simple model. Fig. 27 shows the multi-physical coupled response of a RC beam under a cyclic load.

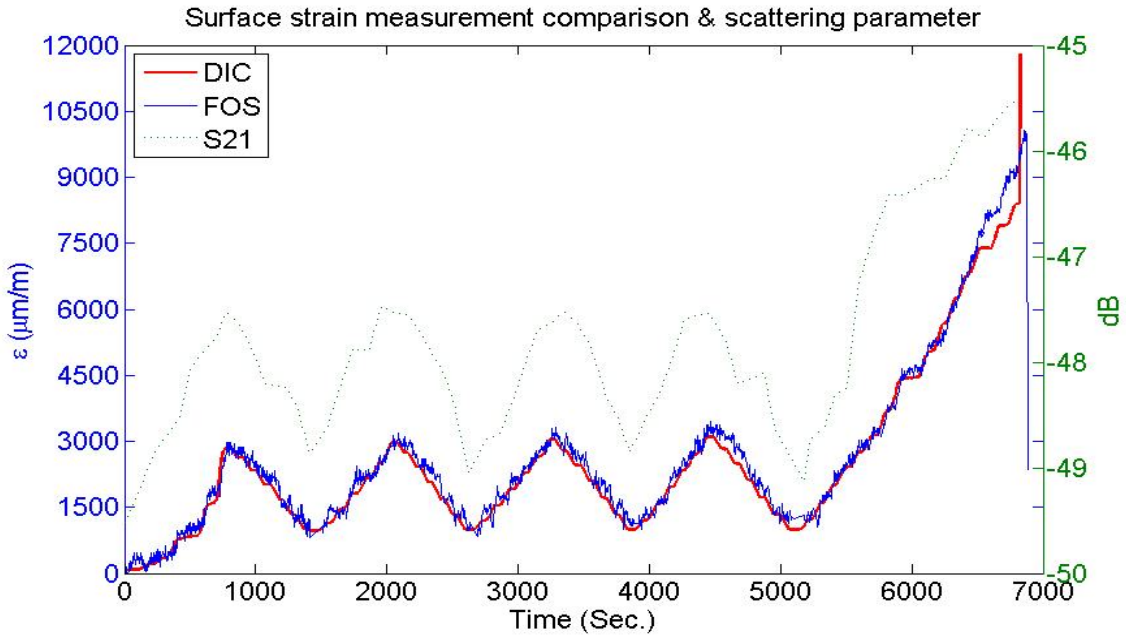

Fig. 27 Coupling of CWIR, DIC and FOS measurements of a laboratory RC beam under cyclic loading

RECOMMENDATIONS

From our research activities and findings, the following recommendations are made.

- Distant radar inspection of RC structures shows promising potential in the subsurface steel rebar detection. Radar imaging also improves the detectability of electromagnetic sensors, while the need to extend the traveling distance of radar (or the level of radar motion) is strongly suggested.
- There is a trade-off between the traveling distance of radar and the level of background electromagnetic noise. The longer distance the radar travels, the better the radar resolution but the more electromagnetic noise can be expected. The quantitative analysis of this trade-off must be carried out by considering the characteristics of background electromagnetic noise of individual sites.

- From our more than 9-month field experiment, DIC appears to be a robust long-term monitoring tool for predicting the concrete cracking potential. The need for physically deploying dot-pattern onto the surface of RC structures is proved to be no longer necessary, also from our field tests. A laser pattern projector is capable of achieving the same result for DIC inspection. However, the performance of nighttime DIC inspection on RC structures is not studied in this project and is recommended for future work.
- It is demonstrated that DIC can provide satisfactory performance on strain/displacement measurement. Therefore, surface-mounted FOS strain sensors can be avoided as long as the surface strain inspection is only needed during daytime.
- Variation of concrete properties due to physical aging and chemical attacks can also affect the performance of CWIR and must be investigated by a comprehensive, systematic study. Although concrete damages like ASR (alkali-silica reaction) were not within the scope of this project, it is important to understand how concrete damages change the radar signal/image of RC structures.

ATTACHMENTS

There are four attachments to this Final Report draft, including:

1. Monte-Carlo simulation of the CWIR sensor
2. FOS laboratory tests
3. Hole drilling test for the DIC sensor and its appendices (a separate document)
4. Field tests of the MRSS technology